Transport and Communications Science Journal, Vol. 77, Issue 4 (05/2026), 594-606

Transport and Communications Science Journal

FORCED VIBRATION ANALYSIS OF VARIABLE THICKNESS MICROPLATE

Dam Vu Son Quyen*

Institute of Technology, Vietnam Defense Industry, Dong Ngac ward, Hanoi, Vietnam

ARTICLE INFO

TYPE: Research Article
Received: 29/11/2025
Revised: 30/12/2025
Accepted: 14/01/2026
Published online: 15/5/2026
https://doi.org/10.47869/tcsj.77.4.19
* *Corresponding author*
Email: damvusonquyen@gmail.com

Abstract. Nowadays, with the development of material science, nano- or microstructures are increasingly of interest in research because of their applications in micro-electromechanical technology, semiconductor chips, or sensors. In this study, the isogeometric approach (IGA) method combining the Mindlin plate hypothesis and the modified couple stress hypothesis is used to analyse the forced vibration of a micro-plate with variable thickness made of materials with variable mechanical characteristics subjected to the effect of different types of dynamic loads. The thickness change of the microplate is considered in two directions with a nonlinear law, while the material characteristics vary with the plate thickness. The model's and method's accuracy are validated by comparing it with results from published studies. Then, the paper surveys the impact of geometric and material coefficient on the transient responses of FG microplate. The research results provide important bases in the design and optimization calculation of micro-electromechanical systems serving the chip and sensor industries.

Keywords: dynamic response, variable thickness, functionally graded material, microplate, isogeometric analysis.

1. BRIEF INTRODUCTION TO RESEARCH DIRECTION

The idea of functionally graded materials (FGMs) was first presented in Japan in 1984 as a novel kind of composite material with characteristics that differ from surface to surface to perform specific tasks, like removing stress concentrations and providing thermal protection from corrosion. Functionally graded (FGs) micro/nano beams and plates are frequently employed in atomic force microscopy and micro and nanoelectromechanical systems (MEMS and NEMS), since the use of

FGMs has recently expanded to the field of micro/nanotechnology [1–3].

Size effects have been seen experimentally in these applications [4] and will be crucial to the possible uses of micro/nano FG beams and plates. Therefore, while forecasting the static and transient reactions of micro/nano FG structures, size effects should be considered. Conventional plate models grounded on continuum mechanics cannot predict size effects due to the lack of inherent length scales. Recently, several size-dependent plate models grounded in size-dependent continuum theories have been developed, including nonlocal hypothesis [5], strain gradient hypothesis [6], couple stress hypothesis [7] , and its modified variant [8]. There have been some studies on microstructures with variable thickness, such as [9–11]. These studies focus on solving the problems of bending and oscillation of the structure. In addition, Thu-Huong et al. [12] used the IGA method to analyze the nonlinear free vibration of microsheet of variable thickness with mechanical characteristics varying in three directions. Ngoc-Anh and co-workers [13] discovered the nonlinear free oscillation behaviors of variable thickness microplates made of FG-GOEAM material based IGA method. The linear vibrational behaviors of multilayer micro-plate structures made of graphene reinforced FG materials resting on viscoelastic and temperature environments were discovered by J. Lawongkerd et al. [14]. Nguyen Chi and coworkers [15] investigated the static bending behavior of FG beams lying on Pasternak medium using an exact analytical solution and Timoshenko beam theory. Dung et al. [16] carried out nonlinear static bending analysis of microsheet lying on imperfect Pasternak medium. The common feature of most of the above studies is that they focus on analyzing the static bending capacity as well as the oscillation of this structure. There are very few studies evaluating the mechanical response of this structure when subjected to dynamic loads. Predicting the behavior of the structure under the effect of dynamic loads plays a very important role in calculating and optimally designing structures working in real environments.

Based on the above analysis, this study proposes a combined model between the IGA method and the Newmark direct integration, based on the Mindlin plate hypothesis and the modified couple stress hypothesis, to analyze the dynamic response of microplates made of variable mechanical characteristics materials with thickness varying in both directions and subjected to dynamic loading. The model is verified by comparing with reliable results in the literature and then used to investigate the impact of coefficient such as thickness variation law, material characteristics, and load type on the dynamic response of the microsheet. The results obtained from this paper can contribute to the calculation, design, and optimization of micro-electromechanical systems serving high-tech industries such as semiconductor chips, energy, sensors, and microprocessors.

2. MODELING AND MATHEMATICAL BASIS

2.1. Variable thickness microplate model

Consider a rectangular FG microplate of variable thickness as shown in Fig. 1. The geometrical dimensions of the microplate, including length L_x , width L_y and thickness is denoted as $h(x,y)$. The microplate is made of a material with varying mechanical properties according to thickness, with the top surface ($z = h/2$) made entirely of ceramic material and the bottom surface ($z = -h/2$) made entirely of metal material. The thickness $h(x,y)$ variation law of the microplate is given to vary non-linearly in the horizontal plane as shown below [13]:

$$h(x,y) = h_0 \left\{1+\gamma_x \left(x/L_x\right)^{\lambda_x}\right\}\left\{1+\gamma_y \left(y/L_y\right)^{\lambda_y}\right\} \quad (1)$$

in which: $\gamma_x, \gamma_y, \lambda_x, \lambda_y$ are the parameters that control the thickness of the microplate and h_0 is the initial thickness of the microsheet structure. The mechanical characteristics of the microsheet material are described as follows [17]:

$$E(\mathrm{z}) = E_m V_m + E_c V_c = E_m + (E_c - E_m)\left(0.5 + z/h(x,y)\right)^{k_z}$$
$$\rho(\mathrm{z}) = \rho_m V_m + \rho_c V_c = \rho_m + (\rho_c - \rho_m)\left(0.5 + z/h(x,y)\right)^{k_z} \quad (2)$$

where: $E(\mathrm{z}), \rho(\mathrm{z})$ are the elastic modulus and density of the plate material, respectively; the indices c and m represent the ceramic and metal components in the material, respectively; k_z represents the material exponent factor.

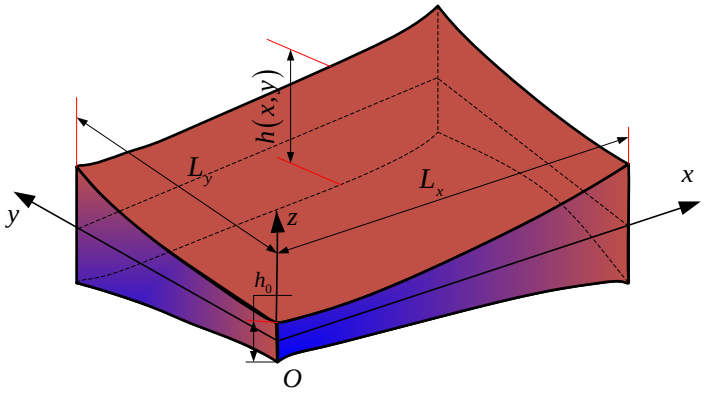

Figure. 1. Model of variable thickness mechanical microplate.

2.2. Dynamic load model

For structures in general and microstructures in particular, during the working process, they are affected by many different types of loads, including dynamic loads. In fact, these types of loads are very complex, such as shock wave loads of explosions, wind loads, impact loads, etc., so it is difficult to represent them with precise mathematical equations. In this paper, four time-varying load forms are used, described by the mathematical formula as below [18]:

$$q(x,y,t) = q_0 F(t) \quad (3)$$

- With rectangular dynamic load:

$$F(t) = \begin{cases} 1 & \text{with } 0 \le t \le t_1 \\ 0 & \text{with } t > t_1 \end{cases} \quad (4)$$

- With triangular dynamic load:

$$F(t) = \begin{cases} 1 - \dfrac{2t}{t_1} & \text{with } 0 \le t \le t_1 \\ 0 & \text{with } t > t_1 \end{cases} \quad (5)$$

- With sinusoidal dynamic load:

$$F(t)=\begin{cases}\sin(\Omega_e t) & \text{with } 0\le t\le t_1\\ 0 & \text{with } t>t_1\end{cases} \tag{6}$$

- With blast dynamic load:

$$F(t)=\begin{cases}e^{-\Omega_e t/t_1} & \text{with } 0\le t\le t_1\\ 0 & \text{with } t>t_1\end{cases} \tag{7}$$

where: t_1 represents the total time of action of external force on the microsheet. In this paper, other values of dynamic load are defined as follows, $t_1=0.5t, \Omega_e=0.5\omega_1$ is the first frequency of microplate.

2.3. Constitutive relationships

Based on Mindlin's plate theory [19], the displacement at any location on the microplate is articulated as follows:

$$\begin{cases}u=u_0+z\varphi_x\\ v=v_0+z\varphi_y\\ w=w_0\end{cases} \tag{8}$$

here: u_0, v_0, w_0 and φ_x, φ_y are the displacement and rotational components to be determined, respectively. The linear strain field of the microplate is delineated as follows:

$$\boldsymbol{\varepsilon}_b=\boldsymbol{\varepsilon}_1-z\boldsymbol{\varepsilon}_2, \boldsymbol{\varepsilon}_s=\boldsymbol{\gamma}_0, \text{ with: } \boldsymbol{\varepsilon}_1=\begin{Bmatrix}\dfrac{\partial u_0}{\partial x}\\ \dfrac{\partial v_0}{\partial y}\\ \dfrac{\partial u_0}{\partial y}+\dfrac{\partial v_0}{\partial x}\end{Bmatrix}, \varepsilon_2=\begin{Bmatrix}\dfrac{\partial \varphi_x}{\partial x}\\ \dfrac{\partial \varphi_y}{\partial y}\\ \dfrac{\partial \varphi_x}{\partial y}+\dfrac{\partial \varphi_y}{\partial x}\end{Bmatrix}, \gamma_0=\begin{Bmatrix}\dfrac{\partial w_0}{\partial x}+\varphi_x\\ \dfrac{\partial w_0}{\partial y}+\varphi_y\end{Bmatrix} \tag{9}$$

Based on Yang's modified stress couple theory [8], the curvature tensor components θ_{ij} is determined as below:

$$\theta_b=\begin{Bmatrix}\theta_{xx}\\ \theta_{yy}\\ \theta_{zz}\\ \theta_{xy}\end{Bmatrix}, \theta_s=\begin{Bmatrix}\theta^1_{xz}\\ \theta^1_{yz}\end{Bmatrix}-z\begin{Bmatrix}\theta^2_{xz}\\ \theta^2_{yz}\end{Bmatrix}, \theta_{xx}=\frac{1}{2}\left(\frac{\partial^2 w_0}{\partial x\partial y}+\frac{\partial \varphi_y}{\partial x}\right), \theta_{yy}=-\frac{1}{2}\left(\frac{\partial^2 w_0}{\partial x\partial y}+\frac{\partial \varphi_x}{\partial y}\right), \tag{10a}$$

$$\theta_{zz}=-\frac{1}{2}\left(\frac{\partial\varphi_y}{\partial x}-\frac{\partial\varphi_x}{\partial y}\right),\theta_{xy}=\frac{1}{4}\left(\frac{\partial^2 w_0}{\partial y^2}-\frac{\partial^2 w_0}{\partial x^2}+\frac{\partial\varphi_y}{\partial y}-\frac{\partial\varphi_x}{\partial x}\right),\theta_{yz}^1=\frac{1}{4}\left(\frac{\partial^2 v_0}{\partial x^2}-\frac{\partial^2 u_0}{\partial x\partial y}\right),$$
$$\theta_{xz}^1=\frac{1}{4}\left(\frac{\partial^2 v_0}{\partial x\partial y}-\frac{\partial^2 u_0}{\partial y^2}\right),\theta_{yz}^2=\frac{1}{4}\left(\frac{\partial^2\varphi_x}{\partial y^2}-\frac{\partial^2\varphi_y}{\partial x\partial y}\right),\theta_{xz}^2=\frac{1}{4}\left(\frac{\partial^2\varphi_x}{\partial x\partial y}-\frac{\partial^2\varphi_y}{\partial x^2}\right) \quad (10b)$$

Based on Hamilton's principle [20], the weak form describing the oscillation of a microsheet of varying thickness is described as follows:

$$\int_S\left(\delta\boldsymbol{\varepsilon}_b^T D_b\boldsymbol{\varepsilon}_b+\delta\boldsymbol{\varepsilon}_s^T D_s\boldsymbol{\varepsilon}_s+\delta\boldsymbol{\theta}_b^T D_{mb}\boldsymbol{\theta}_b+\delta\boldsymbol{\theta}_s^T D_{ms}\boldsymbol{\theta}_s\right)=\int_S q(x,y,t)\delta w_0+\int_S\delta u_b^T H_b u_b \quad (11)$$

in which

$$D_b=\begin{bmatrix}A & B\\ B & E\end{bmatrix},D_{ms}=\begin{bmatrix}P & Q\\ Q & R\end{bmatrix},\{A,B,E\}=\int_{-h(x,y)/2}^{h(x,y)/2}Q_b(1,z,z^2)dz,\ D_s=\frac{5}{6}\int_{-h(x,y)/2}^{h(x,y)/2}Q_s dz,$$
$$\{P,Q,R\}=\int_{-h(x,y)/2}^{h(x,y)/2}Q_{ms}(1,z,z^2)dz,D_{mb}=\int_{-h(x,y)/2}^{h(x,y)/2}Q_{mb}dz,Q_{ms}=\begin{bmatrix}2Gl^2 & 0\\ 0 & 2Gl^2\end{bmatrix} \quad (12)$$

$$Q_b=\begin{bmatrix}c_{11} & c_{12} & 0\\ c_{12} & c_{22} & 0\\ 0 & 0 & c_{66}\end{bmatrix},Q_{mb}=\begin{bmatrix}2Gl^2 & 0 & 0 & 0\\ 0 & 2Gl^2 & 0 & 0\\ 0 & 0 & 2Gl^2 & 0\\ 0 & 0 & 0 & 2Gl^2\end{bmatrix},Q_b=\begin{bmatrix}c_{44} & 0\\ 0 & c_{55}\end{bmatrix}, \quad (13)$$

$$u_b=\begin{Bmatrix}u_0\\ v_0\\ w_0\\ \varphi_x\\ \varphi_y\end{Bmatrix},H_b=\begin{bmatrix}L_1 & 0 & 0 & L_2 & 0\\ & L_1 & 0 & 0 & L_2\\ & & L_1 & 0 & 0\\ & & & L_3 & 0\\ & & & & L_3\end{bmatrix},(L_1,L_2,L_3)=\int_{-h(x,y)/2}^{h(x,y)/2}(1,z,z^2)dz \quad (14)$$

here: l called the length scale factor, this factor characterizes microstructures and explains the cause of the stiffness of the structure.

3. ISOEGOMETRIC METHOD

Based on NURBS functions [21], displacement components u_0, v_0, w_0, φ_x and φ_y of the microplate can be approximately calculated as follows:

$$u_0=\sum_{e=1}^{N_e}\begin{bmatrix}R_e & 0 & 0 & 0 & 0\end{bmatrix}\bar{q}_e=\sum_{e=1}^{N_e}X_e^u\bar{q}_e,v_0=\sum_{e=1}^{N_e}\begin{bmatrix}0 & R_e & 0 & 0 & 0\end{bmatrix}\bar{q}_e=\sum_{e=1}^{N_e}X_e^v\bar{q}_e \quad (15a)$$

$$w_0 = \sum_{e=1}^{N_e} \begin{bmatrix} 0 & 0 & R_e & 0 & 0 \end{bmatrix} \overline{q}_e = \sum_{e=1}^{N_e} X_e^{\,w} \overline{q}_e, \varphi_x = \sum_{e=1}^{N_e} \begin{bmatrix} 0 & 0 & 0 & R_e & 0 \end{bmatrix} \overline{q}_e = \sum_{e=1}^{N_e} X_e^{\,x} \overline{q}_e \tag{15b}$$

$$\varphi_y = \sum_{e=1}^{N_e} \begin{bmatrix} 0 & 0 & 0 & 0 & R_e \end{bmatrix} \overline{q}_e = \sum_{e=1}^{N_e} X_e^{\,y} \overline{q}_e \tag{15c}$$

here: the unknown shape functions and displacement vectors at the control point e are shown by $\boldsymbol{R}_e$ and $\overline{\boldsymbol{q}}_e$, respectively. $N_e = (p+1)(q+1)$ is the number of control points per physical element. p and q are the degrees of the function.

By inserting Eq. (15) into Eq. (11), the this work obtains a general differential equation system describing the oscillation state of the FG microsheet subjected to dynamic load as follows:

$$M\ddot{\overline{q}} + K\overline{q} = F \tag{16}$$

in which: $M = \sum_{e=1}^{Nel} M_e, K = \sum_{e=1}^{Nel} K_e, F = \sum_{e=1}^{Nel} F_e$ are the overall mass matric, overall stiffness matrix and global force vector of the structure respectively, their subcomponents are defined as below:

$$M_e = \int_{S_e} N^T H_b N dxdy, F_e = \int_{S_e} q(x,y,t) X_e^{\,w} dxdy, N = \begin{bmatrix} X_e^{\,u} & X_e^{\,v} & X_e^{\,w} & X_e^{\,x} & X_e^{\,y} \end{bmatrix}^T \tag{17}$$

$$K_e = \int_{S_e} \left(\begin{Bmatrix} B_1 \\ B_2 \\ B_s \end{Bmatrix}^T \begin{bmatrix} A & B & 0 \\ B & E & 0 \\ 0 & 0 & D_s \end{bmatrix} \begin{Bmatrix} B_1 \\ B_2 \\ B_s \end{Bmatrix} + \begin{Bmatrix} B_{ms}^1 \\ B_{ms}^2 \\ B_{mb} \end{Bmatrix}^T \begin{bmatrix} P & Q & 0 \\ Q & R & 0 \\ 0 & 0 & D_{mb} \end{bmatrix} \begin{Bmatrix} B_{ms}^1 \\ B_{ms}^2 \\ B_{mb} \end{Bmatrix} \right) dxdy \tag{18}$$

$$B_1 = \begin{bmatrix} \dfrac{\partial X_e^{\,u}}{\partial x} \\ \dfrac{\partial X_e^{\,v}}{\partial y} \\ \dfrac{\partial X_e^{\,u}}{\partial y} + \dfrac{\partial X_e^{\,v}}{\partial x} \end{bmatrix}, B_2 = \begin{bmatrix} \dfrac{\partial X_e^{\,x}}{\partial x} \\ \dfrac{\partial X_e^{\,y}}{\partial y} \\ \dfrac{\partial X_e^{\,x}}{\partial y} + \dfrac{\partial X_e^{\,y}}{\partial x} \end{bmatrix}, B_s = \begin{bmatrix} X_e^{\,x} + \dfrac{\partial X_e^{\,w}}{\partial x} \\ X_e^{\,y} + \dfrac{\partial X_e^{\,w}}{\partial y} \end{bmatrix}, B_{ms}^1 = \frac{1}{4} \begin{bmatrix} \dfrac{\partial^2 X_e^{\,v}}{\partial x \partial y} - \dfrac{\partial^2 X_e^{\,u}}{\partial y^2} \\ \dfrac{\partial^2 X_e^{\,v}}{\partial x^2} - \dfrac{\partial^2 X_e^{\,u}}{\partial x \partial y} \end{bmatrix}, \tag{19}$$

$$B_{ms}^{2}=\frac{1}{4}\begin{bmatrix}\dfrac{\partial^{2}X_{e}^{x}}{\partial x\partial y}-\dfrac{\partial^{2}X_{e}^{y}}{\partial x^{2}}\\ \dfrac{\partial^{2}X_{e}^{x}}{\partial y^{2}}-\dfrac{\partial^{2}X_{e}^{y}}{\partial x\partial y}\end{bmatrix},B_{mb}=\begin{bmatrix}\dfrac{1}{2}\left(\dfrac{\partial^{2}X_{e}^{w}}{\partial x\partial y}+\dfrac{\partial X_{e}^{y}}{\partial x}\right)\\ -\dfrac{1}{2}\left(\dfrac{\partial^{2}X_{e}^{w}}{\partial x\partial y}+\dfrac{\partial X_{e}^{x}}{\partial y}\right)\\ -\dfrac{1}{2}\left(\dfrac{\partial X_{e}^{y}}{\partial x}-\dfrac{\partial X_{e}^{x}}{\partial y}\right)\\ \dfrac{1}{4}\left(\dfrac{\partial^{2}X_{e}^{w}}{\partial y^{2}}-\dfrac{\partial^{2}X_{e}^{w}}{\partial x^{2}}+\dfrac{\partial X_{e}^{y}}{\partial y}-\dfrac{\partial X_{e}^{x}}{\partial x}\right)\end{bmatrix} \tag{20}$$

The system of equations is a linear differential system in time. Therefore, in this paper, the programming algorithm on MATLAB platform combined with the Newmark direct integration method has been applied to obtain the transient responses of the microsheet with various boundary conditions [22]. The boundary conditions in the article are denoted and defined as follows: C: clamp connection; S: single support connection. CCCC: four-sided clamp connection plate. SSSS: four-sided single support connection plate. CSCS: plate with alternating clamp and single support connections. CCSS: plate with two adjacent clamp connections and two adjacent single support connections. Similar to the plates with the above characters.

4. SOME NUMERICAL RESULTS AND COMMENTS

To produce the dynamic response results, the input coefficient of the microsheet structure are given as follows (when investigating, some parameters will change; the remaining parameters are kept the same): $h_0=17.6\mu m, L_x=10h_0, L_y=10h_0, l=0.2h_0, k_z=1, \gamma_x=0.1,$ $\gamma_y=0.3, \lambda_x=1.5, \lambda_y=0.5$. Variable mechanical properties materials made of metallic materials Al and ceramic materials Al_2O_3 have mechanical properties is $E_c=380GPa,$ $v_c=0.3, \rho_c=3.8\,g/cm^3, E_m=70GPa,\ v_m=0.3, \rho_m=2.7\,g/cm^3$. The dynamic responses including vertical deflection $w_1(t)$ and phase trajectory $w_1(t)-v_1(t)$ over time at the center point of the microplate are presented as numerical result plots as shown below.

$$\Omega_1=\omega_1\frac{L_x^2}{h_0}\sqrt{\frac{\rho_c}{E_c}}, w_1(t)=w_0\left(\frac{L_x}{2},\frac{L_y}{2}\right)\frac{100E_ch_0^3}{q_0L_x^4}, v_1(t)=v_0\frac{E_ch_0^3t_{max}}{q_0L_x^4}, t_{max}=5\sqrt{\frac{\rho_cL_x^4}{E_ch_0^2}} \tag{21}$$

where: ω_1 is the first frequency of the non-uniform FG microsheet.

4.1 Verify accuracy

First, the convergence of the IGA method for the natural oscillation frequency Ω_1 of the FG microplate is presented in Table 1. The number of control points varied from 3x3 to 15x15 with the degree of the function *p(q)* taken as 2, 3, 4. The results show that the oscillation frequency converges quickly when *p(q)*=4 and the number of control points is greater than 7x7. Based on the computing speed of the computer and based on research [22], the number of

control nodes is 11x11 and the element degree is *p(q)=4* which is used for all the investigations in this paper.

Table 1. The convergence of dimensionless natural frequencies Ω_1 of non-uniform thickness microsheet.

		number of control points						
BCs	*p*(*q*)	3x3	5x5	7x7	9x9	11x11	13x13	15x15
SSSS	2	5.7326	5.6427	5.6194	5.6100	5.6052	5.6025	5.6008
	3	5.5997	5.5962	5.5958	5.5958	5.5958	5.5957	5.5957
	4	5.5959	5.5957	5.5957	5.5957	5.5957	5.5957	5.5957
CCCC	2	12.7458	10.5710	10.1284	9.9558	9.8692	9.8191	9.7874
	3	9.8304	9.7393	9.7152	9.7044	9.7044	9.7044	9.7044
	4	9.7307	9.7077	9.6978	9.6978	9.6978	9.6978	9.6978

The survey object is a square plate with length $L_x = 0.45m$, width $h = 0.045m$, and mechanical parameters of the material include: E = 3 GPa, $\nu = 0.34$, and $\rho = 1200\,kg/m^3$. The plate is subjected to a time-varying triangular load with maximum intensity $P_m = 500kPa$ and duration of action T_p = 0.01s. The results of displacement at the centre of the plate over time are compared with the analytical solution by the Navier method in Song's work [23] and are shown in Fig. 2 with the largest deflection of 0.15 mm. The agreement between the two results confirms the correctness and reliability of the calculation model used in this study.

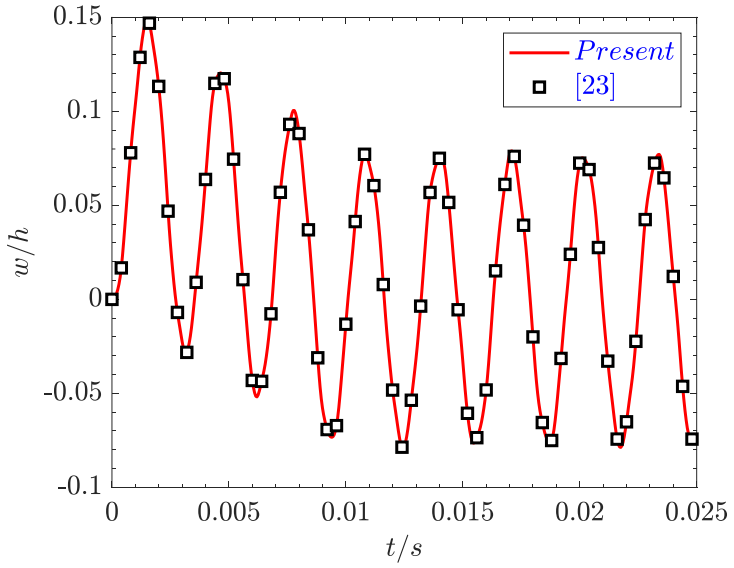

Figure. 2. Comparison of displacement between plates over time.

4.2. Some results of survey

Firstly, the impact of the length-scale factor l on the deflection responses and phase trajectories of the microplate is depicted in Fig. 3. It is easy to see that, as the ratio l/h_0 increases, the deflection amplitude over time decreases, which is explained by the fact that at

the micrometer scale, the factor l plays an important role in increasing the strain energy of the structure, and thus the considered structure will be stiffer. It should be noted here that the time of the external force is only 0.5 times the time of the survey. Therefore, after the external force, the structure will oscillate freely. Moreover, due to the assumption that the working structure is not subject to the effect of the resistance force, so after removing the applied load, the structure will oscillate freely periodically over time. Looking at Fig.3, we can also see that, when the stiffness of the plate is improved and stiffer, the oscillation period of the deflection amplitude also decreases and along with that, the time for the structure to reach the maximum value is also faster.

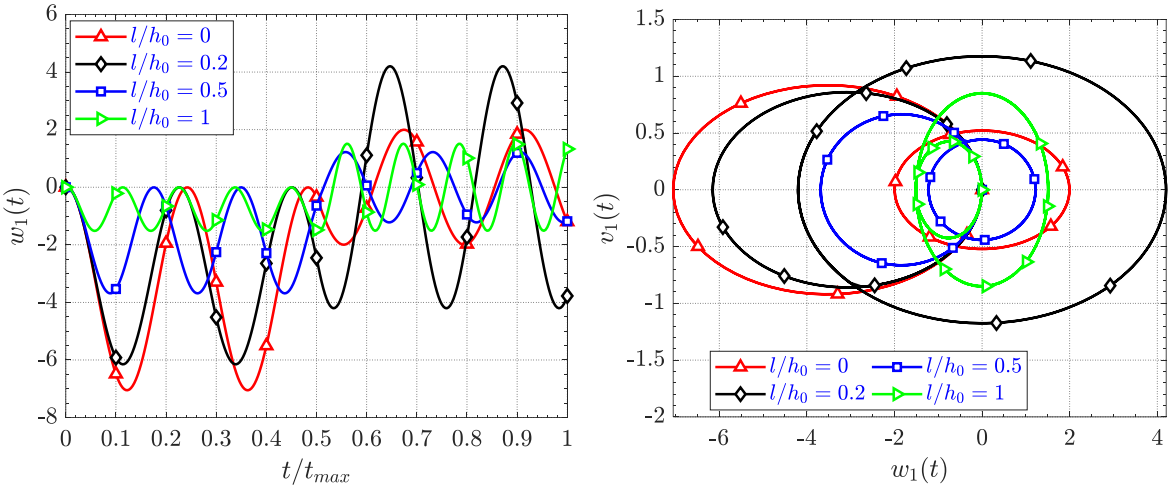

a) deflection b) phase trajectory

Figure. 3. Impact of length scale factor l on dynamic response of FG microplate under rectangular load (SSSS).

Next, the influence of the material exponential coefficient k_z on the deflection response of the microplate subjected to `a sinusoidal` load is described in Fig. 4. In this investigation, the coefficients are investigated with 4 values: 0, 0.5, 1 and 10, along with the boundary condition CCCC. The results show that, during the time of action of the sinusoidal external force, when the coefficient k_z increases, it makes the deflection amplitude value increase, and the time to reach the maximum deflection value also increases. More specifically, the time to reach the maximum deflection value at $k_z = 10$ is $1.08\, t_{\max}$, while the time to reach the maximum deflection value at $k_z = 0$ is only $0.7\, t_{\max}$. Also note that, when the external force is removed, when the system oscillates freely, the amplitude of free oscillation at this time, in addition to being affected by the internal structure itself, also depends on the time of removing the external force. If the accumulated energy when removing the external force is still large, it will continue to oscillate greatly, and when the time of removing the external force is small, the amplitude of free oscillation will be small.

Finally, the effects of taper coefficients γ_x, γ_y and thickness change law control λ_x, λ_y on the deflection responses of the microplate under triangular loading and blast loading are depicted in Fig. 5 and Fig. 6, respectively. In this survey, the coefficients γ_x, γ_y are given 4 values respectively: 0, 0.1, 0.3 and 0.5; while the coefficients λ_x, λ_y are surveyed at the values of 0, 0.5, 1 and 5. From the response results, it is shown that, when the taper coefficients γ_x, γ_y

increase, the deflection amplitude will decrease, which is completely understandable because the increase in coefficients γ_x, γ_y will make the plate thicker and therefore the structural stiffness it brings will increase. In addition, the increasing thickness control coefficient λ_x, λ_y increases the deflection, so the micro-plate structure will be softer. From here, we can see that the thickness and the plate thickness change rule really affect the structure's vibration process significantly. Therefore, for each specific structure, calculating and choosing the thickness and thickness rule will help optimize the cost as well as the durability during the structure's operation.

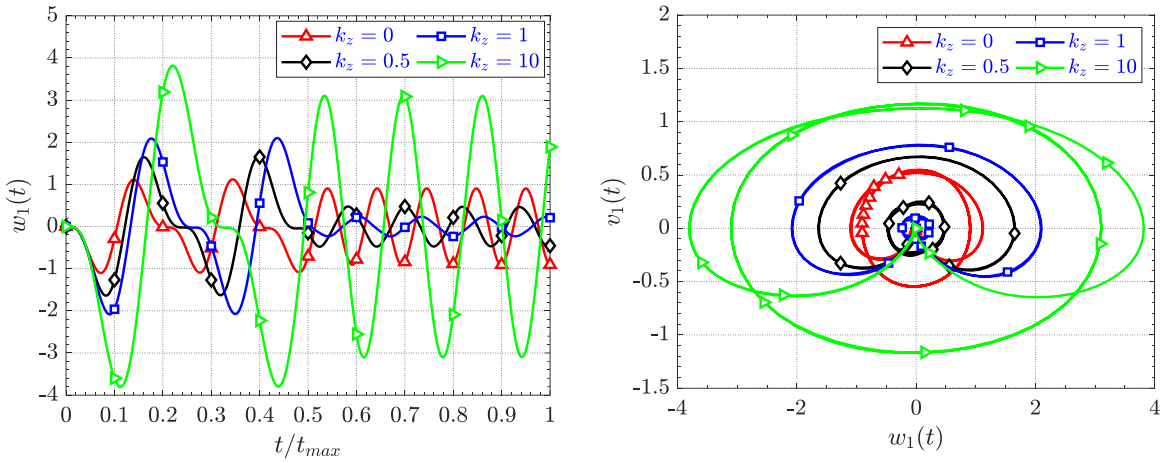

a) deflection b) phase trajectory

Figure. 4. Impact of material exponent factor k_z on deflection response of FG microplate under sinusoidal load (CCCC).

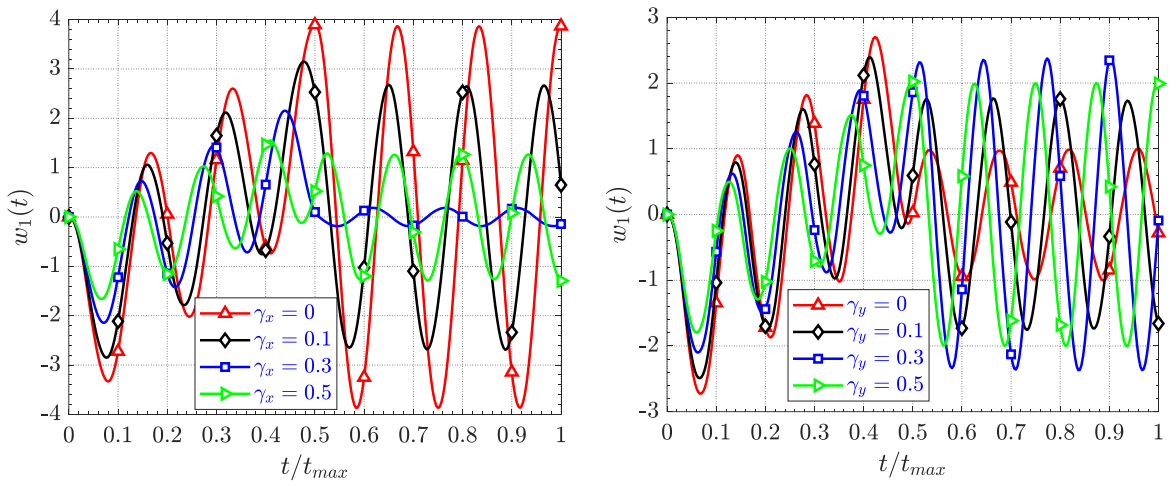

a) CSCS b) CCCC

Figure. 5. Impact of taper coefficient γ_x, γ_y on deflection response results of FG microplate under triangular load.

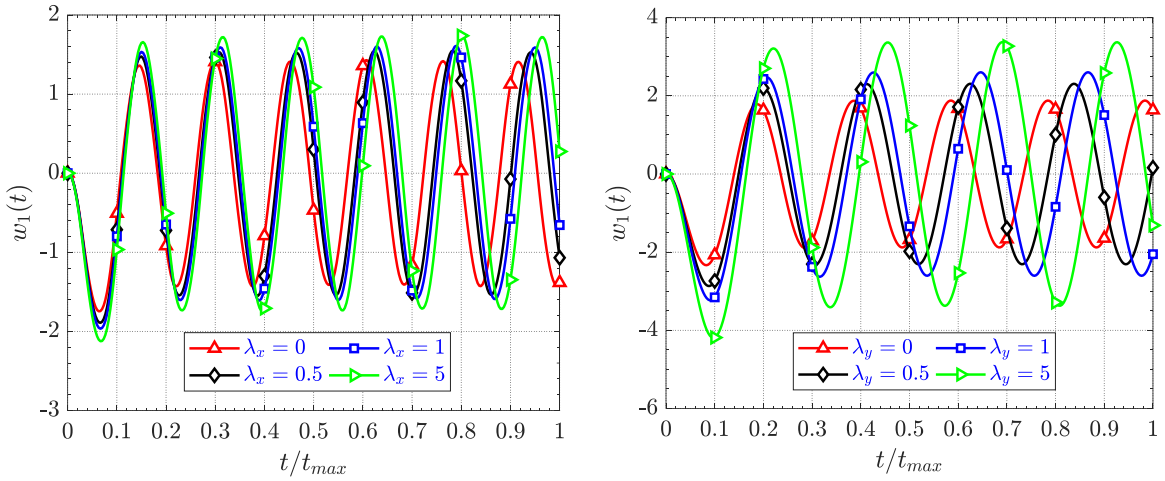

a) CCSS b) SSSS

Figure. 6. Impact of thickness rule control coefficient λ_x, λ_y on deflection response results of FG microplate under blast load.

5. CONCLUSION

Based on the IGA method, modified stress couple theory, and Mindlin plate theory, this paper has analyzed the forced oscillation response of FG microplate with non-uniform thickness. The paper has established a set of calculation programs on MATLAB software and verified them through reliable numerical comparison. Through a series of numerical investigations, the paper finds that the length scale factor l has a significant impact when the structure has a micrometer size and is neglected when the structure size increases to the macroscale; the magnitude of the dynamic responses will increase when the material exponent factor k_z increases. Meanwhile, the increasing taper coefficients γ_x, γ_y make the microplate stiffer and thus reduce the dynamic responses of the microplate. On the contrary, the increasing thickness control coefficients λ_x, λ_y increase the dynamic response values. In addition, the dynamic response results are also highly dependent on different boundary conditions. These results can be useful references in the calculation and design of micro-electromechanical structures, serving engineering industries requiring high technology, such as semiconductors, chips, sensors, and biomedicine.

REFERENCES

[1]. Y. Fu, H. Du, W. Huang, S. Zhang, M. Hu, TiNi-based thin films in MEMS applications: A review, Sensors and Actuators A: Physical, 112 (2004) 395–408. https://doi.org/10.1016/j.sna.2004.02.019

[2]. A. Witvrouw, A. Mehta, The Use of Functionally Graded Poly-SiGe Layers for MEMS Applications, Materials Science Forum, 492–493 (2005) 255–260. https://doi.org/10.4028/www.scientific.net/msf.492-493.255

[3]. Z. Lee, C. Ophus, L.M. Fischer, N. Nelson-Fitzpatrick, K.L. Westra, S. Evoy, V. Radmilovic, U. Dahmen, D. Mitlin, Metallic NEMS components fabricated from nanocomposite Al-Mo films, Nanotechnology, 17 (2006) 3063–3070. https://doi.org/10.1088/0957-4484/17/12/042

[4]. N.A. Fleck, G.M. Muller, M.F. Ashby, J.W. Hutchinson, Strain gradient plasticity: Theory and experiment, Acta Metallurgica Et Materialia, 42 (1994) 475–487. https://doi.org/10.1016/0956-7151(94)90502-9

[5] A.C. Eringen, Nonlocal polar elastic continua, International Journal of Engineering Science, 10 (1972) 1–16. https://doi.org/10.1016/0020-7225(72)90070-5
[6]. D.C.C. Lam, F. Yang, A.C.M. Chong, J. Wang, P. Tong, Experiments and theory in strain gradient elasticity, Journal of the Mechanics and Physics of Solids, 51 (2003) 1477–1508. https://doi.org/10.1016/S0022-5096(03)00053-X
[7]. Tiersten H.F., R.D. Mindlin, Effects of couple-stresses in linear elasticity, Wear 6 (1963) 243. https://doi.org/10.1016/0043-1648(63)90083-8
[8]. F. Yang, A.C.M. Chong, D.C.C. Lam, P. Tong, Couple stress based strain gradient theory for elasticity, International Journal of Solids and Structures, 39 (2002) 2731–2743. https://doi.org/10.1016/S0020-7683(02)00152-X
[9]. Q.H. Pham, P.C. Nguyen, V.K. Tran, Effects of hygro-thermal environment on dynamic responses of variable thickness functionally graded porous microplates, Steel and Composite Structures, 50 (2024) 563–581. https://doi.org/10.12989/scs.2024.50.5.563
[10]. D.T.M. Cuong, T. V. Do, N.V. Dung, Effect of novel elastic foundations on the thermal buckling behavior of organic nanobeams, Mechanics Based Design of Structures and Machines, 54 (2026) 2556241. https://doi.org/10.1080/15397734.2025.2556241
[11]. T.D. Van, M.C. Van, V.M. Phung, V.N.D. Anh, Mechanical responses of nanoplates resting on viscoelastic foundations in multi-physical environments, European Journal of Mechanics - A/Solids, 106 (2024) 105309. https://doi.org/10.1016/j.euromechsol.2024.105309
[12] T.H.N. Thi, V.K. Tran, V.K. Trai, L. Hoai, An IGA approach for linear and nonlinear free vibration of tri-directional functionally graded porous microplate in nonlinear high-temperature environment with nonlinear variable thickness, Thin-Walled Structures, 217 (2025) 113784. https://doi.org/10.1016/j.tws.2025.113784.
[13]. V.N. Anh, T. Van Ke, N.T.T. Huong, N.T. Hue, P.H. Tu, Nonlinear Free Vibrations of Functionally Graded Graphene Origami-Enabled Auxetic Metamaterial Skew-microplates with Variable Thickness Using Isogeometric Analysis, Defence Technology, 57 (2025) 85-108. https://doi.org/10.1016/j.dt.2025.09.024.
[14] J. Lawongkerd, P. Roodgar Saffari, T. Jearsiripongkul, C. Thongchom, S.O. Ismail, P.R. Saffari, S. Keawsawasvong, Vibration characteristics of multilayer functionally graded microplates with variable thickness reinforced by graphene platelets resting on the viscoelastic medium under thermal effects, International Journal of Thermofluids, 22 (2024) 100611. https://doi.org/10.1016/j.ijft.2024.100611.
[15]. T. Nguyen Chi, H. Vu Van, H. Le Hong, H. Nguyen Huu, T. Pham Duc, T. Dao Minh, Study of static bending of functionally graded beams using analytical method, Transport and Communications Science Journal, 76 (2025) 928–938. https://doi.org/10.47869/tcsj.76.7.1.
[16]. N.T. Dung, L.M. Thai, T. Van Ke, T.T.H. Huyen, P. Van Minh, Nonlinear static bending analysis of microplates resting on imperfect two-parameter elastic foundations using modified couple stress theory, Comptes Rendus: Mécanique, 350 (2022) 121–141. https://doi.org/10.5802/crmeca.105.
[17]. Y.S. Li, E. Pan, Static bending and free vibration of a functionally graded piezoelectric microplate based on the modified couple-stress theory, International Journal of Engineering Science, 97 (2015) 40–59. https://doi.org/10.1016/j.ijengsci.2015.08.009.
[18]. P. Van Minh, T. Van Ke, A Comprehensive Study on Mechanical Responses of Non-uniform Thickness Piezoelectric Nanoplates Taking into Account the Flexoelectric Effect, Arabian Journal for Science and Engineering, 48 (2023) 11457–11482. https://doi.org/10.1007/s13369-022-07362-8.
[19]. H.M. Ma, X.L. Gao, J.N. Reddy, A non-classical Mindlin plate model based on a modified couple stress theory, Acta Mechanica, 220 (2011) 217–235. https://doi.org/10.1007/s00707-011-0480-4.
[20]. Q.H. Pham, P.C. Nguyen, V.K. Tran, Q.X. Lieu, T.T. Tran, Modified nonlocal couple stress isogeometric approach for bending and free vibration analysis of functionally graded nanoplates, Engineering with Computers, 39 (2023) 993–1018. https://doi.org/10.1007/s00366-022-01726-2.
[21]. T.J.R. Hughes, J.A. Cottrell, Y. Bazilevs, Isogeometric analysis: CAD, finite elements, NURBS, exact geometry and mesh refinement, Computer Methods in Applied Mechanics and Engineering, 194 (2005) 4135–4195. https://doi.org/10.1016/j.cma.2004.10.008.

[22]. P.H. Tu, T. Van Ke, V.K. Trai, L. Hoai, An isogeometric analysis approach for dynamic response of doubly-curved magneto electro elastic composite shallow shell subjected to blast loading, Defence Technology, 41 (2024) 159–180. https://doi.org/10.1016/j.dt.2024.06.005.
[23]. M. Song, S. Kitipornchai, J. Yang, Free and forced vibrations of functionally graded polymer composite plates reinforced with graphene nanoplatelets, Composite Structures, 159 (2017) 579–588. https://doi.org/10.1016/j.compstruct.2016.09.070.